

BLOOD CHARACTERIZATION FROM PULSATILE BIOIMPEDANCE SPECTROSCOPY

Tao Dai

Systems and Computer Engineering, Carleton University, Canada
e-mail: tdai@sce.carleton.ca

Andy Adler

Systems and Computer Engineering, Carleton University, Canada
e-mail: adler@sce.carleton.ca

1 INTRODUCTION

The bioimpedance measurements in humans have been receiving considerable attentions during the past two decades because of several advantages, such as low cost, easy application, non-invasiveness and on-line monitoring. The original bioimpedance technique was bioelectrical impedance analysis (BIA). Within a decade, this technique evolved into the more advanced technique known as bioelectrical impedance spectroscopy (BIS), also called multiple-frequency bioimpedance analysis (MFBIA). BIS applies multi-frequency stimulations to measure body impedance. This technique has been widely used for many applications, such as:

- Body fluid measurement[1][2]. This method estimates extracellular fluid (ECF), intracellular fluid (ICF) and total body water (TBW);
- Tissue volume change. A typical application of this type is the impedance plethysmography[3].
- Tissue characterization. These techniques are mostly based on Cole-Cole model in terms of Cole-Cole impedance parameters[4]. *e.g.* in [5], normal and ischemic tissues are differentiated by comparing R_0 and f_c . in [6], Zhao et al. calculated plasma resistance, intracellular resistance and cell membrane capacitance of blood using three measuring frequencies.

Characterization of blood bioimpedance properties is of importance for the development of methods estimating some clinical diagnostic indices such as haematocrit, glucose level, hydration, etc. The ability to make *in vivo* measurements would be a great advance; however, Current bioimpedance spectroscopy measurements of blood are either *in vitro*[6][7], or are performed on a body appendage and thus represent a combined measurement of all tissues in the measuring field[8], rather than the blood impedance value. In this paper, we propose a novel approach to measure blood impedance *in vivo* by analyses of data from the cardiac induced pulsatile impedance signal. Pulsatile data are used to fit a non-linear model, from which arterial blood parameters are separated from those of the surrounding tissues.

2 METHODS

We consider a tetrapolar impedance sensor applied to an index finger or between index and middle fingers so that an alternating current enters finger from two injection electrodes and the voltage is measured between two detection

electrodes. The physiological structure of this compartment is relatively simple compared with other measuring sites (*e.g.* chest) and can be approximated with a cylindrical model describe as Fig. 1.

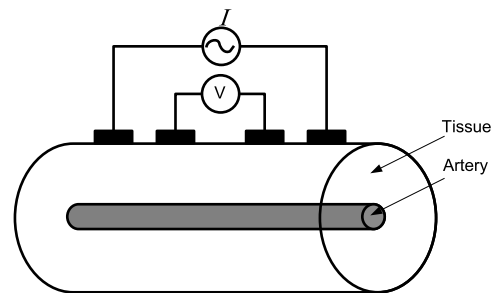


Figure 1. A tetrapolar BIS sensor is applied on a finger segment, modeled as a cylindrical model which contains a uniform blood and tissue compartment.

Arterial expansion during systole increases its cross section area from S_a to $S_a + \Delta S_a$ and the arterial impedance of this segment decreases correspondingly from Z_a to $Z_a - \Delta Z_a$. The fractional variation is thus $\Delta Z_a/Z_a = -\Delta S_a/S_a$. This impedance signal varies with the same frequency as the ECG signal but delayed phase. For simplicity, we use a sinusoidal wave to simulate the real pulsatile wave during modeling (Fig. 2).

In order to build a computational model, we categorize finger tissues into two groups: 1. *Tissue*, which includes everything except arterial blood (ie. muscle, fat, interstitial fluid, venous and capillary blood), and 2. *Arterial blood*. There are two states for arterial blood volume: 1) *Diastole*: arterial blood volume is minimum, and 2) *Systole*: maximum arterial expansion. Based on analysis above, the pulsatile bioimpedance model of a finger can be described as three electrical components in parallel (Fig. 3).

The pulsatile impedance measurements Z_d and Z_s (Fig. 2) originate from the tissue model (Fig. 3) where tissue and arterial blood are represented by impedance Z_I and incremental blood is represented by impedance Z_{II} . During diastole, $Z_d = Z_I$, while during systole, $Z_s = Z_I || Z_{II}$. During the transition from systole to distribution, Z_{II} increases as the incremental blood leaves the arteries.

The impedance spectral data are fitted to the Cole-Cole

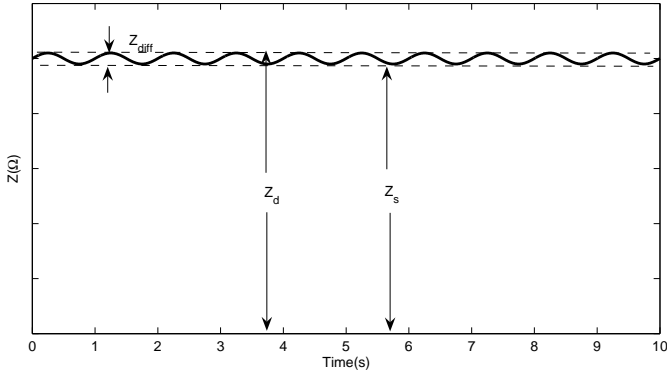


Figure 2. An illustration of the pulsatile impedance wave at a measuring frequency. Z_d : impedance (upper dash line) corresponding to the heart diastole; Z_s : impedance (lower dash line) corresponding to the maximum arterial expansion during heart systole; Z_{diff} : The difference between Z_d and Z_s

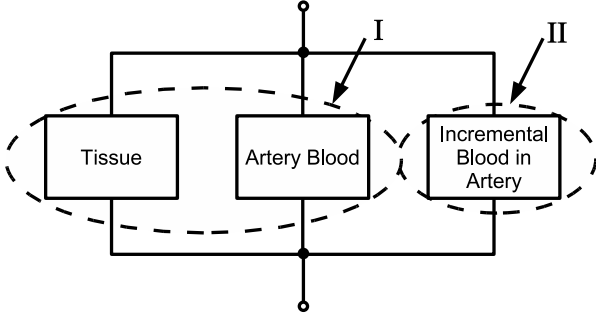


Figure 3. The finger measured is modelled as three parallel impedances. Tissue and arterial blood are grouped as part I (with impedance Z_I), while the incremental blood in the artery is part II (with impedance Z_{II}).

equation [4],

$$Z(f) = R_\infty + \frac{\Delta R}{1 + j(f/f_c)^{1-\alpha}} \quad (1)$$

where R_∞ is the impedance at infinite frequency; $\Delta R = R_0 - R_\infty$, where R_0 is the impedance at zero frequency; f_c is the characteristic frequency of the tissue or model under analysis; α is the constant that characterizes the Cole distribution function. Data are fitted using Levenberg-Marquardt (LM) nonlinear regression algorithm[9]. The resulting model parameter vector for each tissue group is $m = [R_0, \Delta R, f_c, \alpha]$.

The Cole-Cole curve of incremental blood (part II, in Fig. 3) is calculated as follows:

1. From BIS measurements at diastole, we obtain the Cole-Cole curve parameters of $Z_d(f) = Z_I$;
2. From measurements at systole, we obtain the parameters of $Z_s(f) = Z_I \parallel Z_{II}$.

3. The incremental blood impedance spectral $Z_{ib}(f) = Z_{II}$ is calculated by

$$Z_{ib}(f) = \frac{Z_d(f)Z_s(f)}{Z_d(f) - Z_s(f)} \quad (2)$$

which is derived from the parallel relationship illustrated by Fig. 3. The calculated $Z_{ib}(f)$ is blood-related only.

Of the Cole-Cole parameters obtained above, R_0 and R_∞ are geometry-related which are sensitive to body segment dimension changes, electrode movement, and blood pressure changes, etc; f_c is relatively stable against body segment geometrical variations; α is insensitive to tissue property variation[5]; Therefore, f_c is an appropriate candidate for characterizing blood bioimpedance properties. (R_0 , R_∞ , ΔR and the ratio R_0/R_∞ are also helpful provided with careful measurements and calibrations)

3 METHODS: EXPERIMENTAL

A biologic tissue phantom was built. A piece of skinned porcine meat (with size $28\text{cm} \times 14\text{cm} \times 4\text{cm}$) was taken from fridge (cool storage) and placed in room environment (24°C and 64% humidity) at least six hours in order to reach equilibrium at room temperature. A groove (length=25cm, width=height=2cm) was cut at the position which was about one third of the meat width. A strip of porcine liver, with approximately similar size to the groove, was filled in the groove (Fig. 4). Initially, BIS data were measured from this liver strip and Cole-Cole parameters were calculated as the standard to be compared with those of estimated.

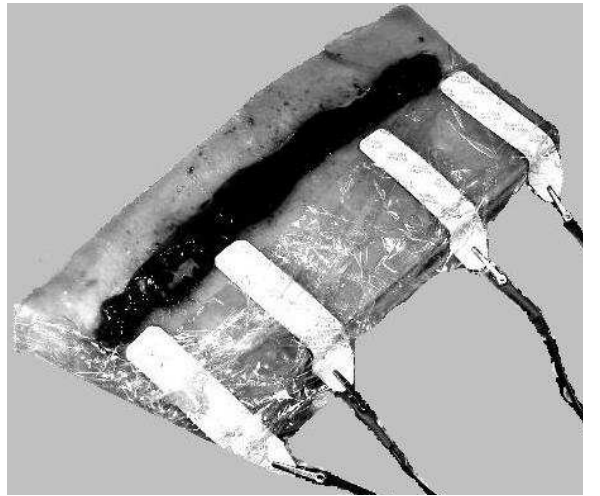


Figure 4. Tissue phantom: porcine meat with liver filling. A tetrapolar BIS sensor is applied.

The goal of this experiment is to validate the approach developed in this paper. From two sets of BIS data of the phantom (measured on porcine base with and without liver filling), we try to figure out the bioelectrical properties of the liver. This is to simulate the corresponding experiment on human finger: Once being provided two sets of BIS data measured on finger (with and without arterial expansion),

we can calculate the bioelectrical properties of the artery blood.

Four IS4000 skin electrodes were placed on the meat, illustrated as Fig. 4, with equidistance. The inner pair were voltage sensors and the outer pair were current injectors, respectively. BIS data were collected by an impedance analyzer (*Xitron 4200 ECF-ICF Bioimpedance Analyzer*) whose spectral sweeps from 5kHz to 1Mhz (50 frequencies, logarithmically linear distributed). The inductive effect, illustrated as the sub-ripple at the high frequency end (Fig. 5(b)5(c)), could be observed in many real measurements even on homogenous tissues[10]. In our measurements, this effect was also observed above 400kHz. Although this additional effect could still be fitted well by using ECFC model ([10]), we chose only 40 frequencies from start (5kHz to 339kHz) to avoid this effect for the sake of a fast and accurate curve fitting.

4 RESULTS

Illustrated in Fig.5(a), two BIS measurements (each was the ensemble average of ten consecutive sweeps), $Z_{base}(f)$ with and without liver filling, were made and the estimated liver Cole-Cole curve was illustrated in Fig.5(c), marked as *. By fitting this curve using a 1st order Cole-Cole model (Fig.5(c), solid line), the liver's Cole-Cole parameters were calculated and compared with those of the previously measured original liver (Fig.5(b), ensemble average of ten consecutive sweeps). Provided the original Cole-Cole model parameters $m_0 = [R_0, \Delta R, f_c, \alpha]$ and the estimated parameters \hat{m} , their corresponding error was calculated through $err = (|\hat{m} - m_0|) ./ m_0 \times 100\%$.

Listed in Table I, three pieces of skinned porcine meat (denoted as 1,2,3) were tested as phantom bases and each had three strips of liver as fillings (denoted as a,b,c). Results were obtained from nine experiments. The average error (μ_e) of $[R_0, \Delta R, f_c, \alpha]$ is [22.35%, 15.85%, 5.99%, 22.79%], respectively. Compared with other parameters, f_c has a much lower error level and a much narrower standard deviation. This outcome verifies experimentally that f_c is a reliable parameter to characterize blood bioelectrical property *in vivo*. Errors originate from multi-sources, such as imperfect contact between phantom bases and fillings, inconsistent geometric states of fillings (twist, stretch, etc). For the purpose of reducing parameter errors, liquid fillings, such as fresh animal/human blood, blood-mimic fluid etc, are suggested for further research.

5 DISCUSSION

This paper introduces a method to measure arterial blood impedance from pulsatile blood impedance measurements. This technique offers the advantage that, in term of physiology, the pulse curve is generated from a homogeneous medium – blood; Therefore parameters of this curve (such as f_c) can be more representative for blood characterization compared with those from curves such as $Z_a(f)$ or $Z_s(f)$ which are generated from multi-tissues due to heterogeneity

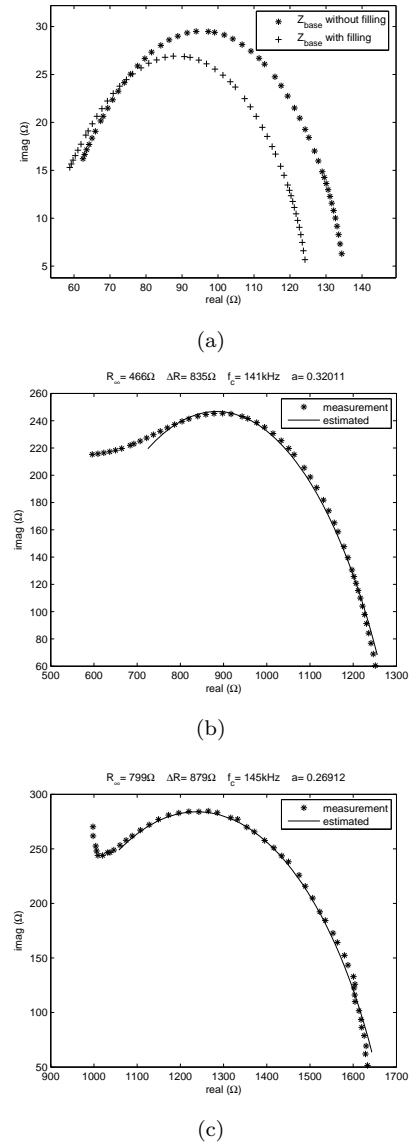


Figure 5. (a) Cole-Cole curve of $Z_{base}(f)$ without and with liver filling, illustrated as '*' and '+', respectively; (b) The original $Z_{liver}(f)$ measured in advance is fitted in a 1st order Cole-Cole model; (c) estimated $Z_{liver}(f)$ is fitted in a 1st order Cole-Cole model.

in the measuring field.

The disadvantage of pulse curve is that, in real measurements, the pulsatile amplitude is only a small fraction (10% or less) of the noise amplitude which introduces impediments to measure pulsatile amplitude accurately. In order to overcome this, high sampling rates and/or additional signal processing approaches are required which increase computational complexities.

Some previous work is related to the method we propose. Yamakoshi et al.[11] showed that the changes in the admittance produced by pulsatile in the human finger dipped in

TABLE I
Estimated (\hat{m}) v.s Original (m_0) Cole-Cole Parameters

		$R_0(\Omega)$			$\Delta R(\Omega)$			$f_c(kHz)$			α		
		m_0	\hat{m}	err(%)	m_0	\hat{m}	err(%)	m_0	\hat{m}	err(%)	m_0	\hat{m}	err(%)
1	a	1682	1530	9.04	1010	1003	0.69	157	141	10.2	0.304	0.261	14.0
	b	2086	1512	27.5	1277	1041	18.5	155	162	4.52	0.319	0.261	18.2
	c	1302	1678	28.9	835	878	5.15	140	145	3.57	0.320	0.269	15.9
2	a	1557	2076	33.3	964	943	2.18	189	157	16.9	0.301	0.251	16.7
	b	1796	1986	10.58	1185	854	27.9	149	133	10.7	0.329	0.233	29.2
	c	1369	1545	12.9	918	886	3.49	182	181	0.55	0.294	0.276	6.12
3	a	1651	1273	22.9	1455	770	47.1	149	150	0.67	0.438	0.316	27.8
	b	1535	2028	32.1	875	668	23.7	193	195	1.04	0.263	0.153	41.9
	c	2088	1590	23.9	1279	1100	14.00	155	164	5.81	0.317	0.206	35.0
error mean $\mu_e(\%)$		22.35			15.85			5.99			22.79		
error std $\delta_e(\%)$		9.30			15.32			5.58			11.41		

the electrolyte vanishes when the conductivity of the electrolyte is equal to that of the blood. However, this method is limited by strict experimental conditions. Brown et al.[8] tried to characterize cardiac related impedance wave measured in the chest and found contradictions while comparing resulting cole-cole parameters with those of blood. They demonstrated that the cardiac related impedance wave was not from blood only but a structure like "blood-tissue" parallel pair and this impedance spectrum could be misleading if being directly used for blood characterization.

The measuring site can be extended to, *e.g.* forearm, with a similar model presented in this paper. For this case, proper blood pooling can be applied to resemble pulsatile behavior within a finger compartment. Similar work can be found from Khan et al.[12] who carried out blood pooling on human calf to check bioelectrical variations.

In conclusion, we proposed a novel technique to calculate *in vivo* properties of arterial blood based on measurements of the cardiac induced pulsatile BIS signal. The measured pulse curve is fitted using nonlinear curve fitting method and a simple first order Cole-Cole model. This method may potentially allow simplified measurement of blood parameters for many biomedical monitoring applications and clinical diagnoses. However, because of noise levels encountered in real measurements, the methodology of obtaining accurate pulse data is a main concern for the future research and development.

ACKNOWLEDGMENTS

This work is supported by a grant from NSERC Canada.

REFERENCES

- [1] Siconolfi SF, Gretebeck RJ, Wong WW, Pietrzyk RA, Suire SS, "Assessing total body water from bioelectrical response spectroscopy", *J Appl Physiol*, 82:704–710. 1997.
- [2] Thomas BJ, Cornish BH, Ward LC "Bioelectrical impedance analysis for measurement of body fluid volumes: A review", *J Clin Eng*, 17:505–510, 1992.
- [3] Nyboer J. *Electrical impedance plethymography*. (2nd ed), Springfield, IL: Thomas, 1970.
- [4] Cole KS, Cole RH, "Dispersion and absorption in dielectrics. I. alternating current characteristics", *J Chem Phys*, 48:341-351, 1941.
- [5] Casas O, Bragos R, Riu RJ, Rosell J, Tresanchez M, Warren M, Rodriguez-Sinovas A, Carrena A, Cinca J, "in vivo and in situ ischemic tissue characterization using electrical impedance spectroscopy", *Ann NY Acad Sci*.20;873:51-8.1999.
- [6] Zhao TX, Jacobson B, Ribbe T, "Triple-frequency method for measuring blood impedance," *Physiol Meas*, 14:145–156, 1993.
- [7] Alison JM, Sheppard RJ, "Dielectric properties of human blood at microwave frequencies", *Phys Med Biol*, 38,971–8, 1993.
- [8] Brown BH, Barber DC, Morice AH, Leathard AD, "Cardiac and respiratory related electrical impedance changes in the human thorax", *IEEE Trans Biomed Eng*, 41:729–34, 1994.
- [9] Moré JJ, "The Levenberg-Marquardt algorithm: implementation and theory," *Numerical Analysis*, ed. G. A. Watson, Lecture Notes in Mathematics 630, Springer Verlag, pp. 105-116, 1977.
- [10] Lafargue AL, Cabrales LB, Larramendi RM, "Bioelectrical parameters of the whole human body obtained through bioelectrical impedance analysis", *Bioelectromagnetics*, 23:450–454, 2002.
- [11] Yamakoshi K, Shimazu H, Togawa T, Fukuoka M, Ito H. "Non-invasive measurement of haematocrit by electrical admittance plethysmography technique", *IEEE Trans Biomed Eng.*, 27:156-161. 1980.
- [12] Munna Khan, Sujoy K.Guha,"Prediction of electrical impedance parameters for the simulated leg segment of an aircraft pilot under G-stress", *Aviation, Space, and Environmental Medicine*, Vol 73, No.6, June 2002.